
The influence of ionic strength on the binding of a water soluble porphyrin to nucleic acids

Robert F. Pasternack*, Paul Garrity, Bruce Ehrlich, Charles B. Davis, Esther J. Gibbs^{1*}, Glennis Orloff¹, Anna Giartosio² and Carlo Turano²

Department of Chemistry, Swarthmore College, Swarthmore, PA 19081, ¹Department of Chemistry, Goucher College, Towson, MD 21204, USA and ²CNR Center of Molecular Biology, University of Rome, 00185 Rome, Italy

Received 13 March 1986; Revised and Accepted 19 June 1986

ABSTRACT

The ionic strength dependences of the binding of tetrakis (4-N-methylpyridyl)porphine (H₂TMpyP) to poly(dG-dC) and calf thymus DNA have been determined. For the former system the results are typical of other intercalators, i.e., a plot of log K vs log [Na⁺] is linear albeit with a slope which suggests that the "effective charge" of the porphyrin is closer to two than the formal charge of +4. For calf thymus DNA, the binding profile is not completely compatible with the predictions of condensation theory. Whereas the avidity of binding does decrease with increasing [Na⁺] as predicted, of greater interest is the relocation of the porphyrin from GC-rich regions to AT-rich regions as the ionic strength increases.

INTRODUCTION

The binding of small molecular ions (ligands) to DNA continues to be a subject of considerable interest in biochemistry. A theoretical model proposed by McGhee and von Hippel (1) remains the standard method of analyzing titration data for such association reactions although the importance of polyelectrolyte effects is now becoming appreciated (2). The McGhee-von Hippel model, in the absence of cooperativity among ligands, leads to the expression:

$$\frac{r}{m} = K(1 - nr) \left(\frac{1 - nr}{1 - (n-1)r} \right)^{n-1} \quad (1)$$

Here $r = [\text{complex}]/[\text{DNA}]_0$, $m =$ concentration of free (unbound) ligand and K is the association constant obtained, as a rule, from plots of r/m vs. r extrapolated to $r = 0$. In expression (1), n is the total number of binding sites eliminated when a ligand binds to the polymer.

McGhee and von Hippel also included ligand-ligand cooperativity in their model through the introduction of a parameter ω , an equilibrium constant for the transfer of a bound ligand from a site with no neighboring ligands to a site with one

such neighbor (3). Now:

$$\frac{r}{m} = K(1 - nr) \left(\frac{(2\omega - 1)(1 - nr) + r - R}{2(\omega - 1)(1 - nr)} \right)^{n-1} \left(\frac{1 - (n+1)r + R}{2(1 - nr)} \right)^2 \quad (2)$$

with $R = [(1 - (n+1)r)^2 + 4\omega r(1 - nr)]^{1/2}$. Equation (2) reduces to equation (1) in the limit of $\omega \rightarrow 1$.

Stability constants obtained from McGhee-von Hippel (or similar analyses) show a dependence on counterion concentration (for example, $[\text{Na}^+]$). The filament-like DNA structure with regularly placed negative charges along its length gives rise to a counterion condensation layer described by Manning (4,5). Theory predicts (6,7) that for this physical situation $\log K$ will show a linear dependence on $\log [\text{Na}^+]$ as:

$$\frac{\delta \log K}{\delta \log [\text{Na}^+]} = -2n(\phi - \phi^*) - z\phi^* \quad (3)$$

In equation (3), ϕ is the counterion fraction arising from both the condensed ion atmosphere and Debye-Huckel type processes on native DNA; ϕ^* is the counterion fraction on "open" DNA, the cooperative unit involved in the intercalation of small molecules; n , as above, is the number of base pairs involved in the binding site and z is the number of ion pairs in the complex which for small molecules is usually equal to the charge of the ligand. (The concentration of the ligand is assumed to be significantly lower than that of the supporting electrolyte, e.g., sodium chloride.)

The work reported on here was undertaken to determine the influence of the ionic strength on a multivalent intercalating drug, tetrakis(4-N-methylpyridyl)-porphine (H_2TMpyP , Figure 1). This substance carries a 4+ charge at or near neutral pH and has been shown to intercalate into naturally occurring DNA (8) as well as poly(dG-dC) (9). Convenient spectroscopic markers are available to study the interactions of H_2TMpyP with nucleic acids. Intercalation which occurs in GC-rich regions leads to a large bathochromic shift of the Soret band (>20 nm), substantial hypochromicity of the Soret maximum (~40%) and an induced circular dichroism band in the Soret region having negative ellipticity (9). Interaction with AT-regions is of an 'external' type involving at best only partial intercalation into the duplex. For these interactions the Soret band is shifted only 9 nm to 430 nm with 7% hypochromicity and the circular dichroism spectrum involves a single positive band in the Soret region (9). Using these spectroscopic fingerprints we now report on a new phenomenon in ligand binding to DNA, a change in base specificity with ionic strength.

MATERIALS AND METHODS

Poly(dG-dC) was purchased from P-L Biochemicals. The solid was dissolved in 0.8 mM phosphate buffer containing 0.1 mM $\text{Na}_2\text{H}_2\text{EDTA}$ and 10 mM NaCl ($\mu = 0.12 \text{ M}$)

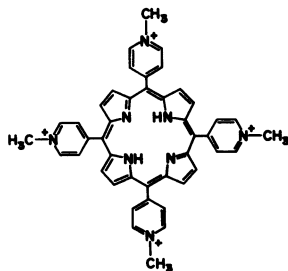


Figure 1. Tetrakis (4-N-methylpyridyl)porphine (H_2TMpyP).

and the solution was dialyzed extensively against a buffer solution of the same composition. The concentration in base pairs/liter of the final stock solution was determined using $\epsilon^{254} = 1.68 \times 10^4 \text{ M}^{-1}\text{cm}^{-1}$.⁽¹⁰⁾ Calf thymus DNA purchased from Sigma Chemical Corp. was purified by standard methods (9) using the same buffer medium described above. Concentrations were determined from $\epsilon^{260} = 1.31 \times 10^4 \text{ M}^{-1}\text{cm}^{-1}$ (11). The pH of all solutions used in the present study was 6.8-7.0.

Tetrakis(4-N-methylpyridyl)porphine tetratosylate was purchased from Man-Win Coordination Chemicals. The anion was exchanged for chloride through use of a Dowex 1-X8 resin supplied by Baker Chemical Company. All other chemicals were obtained from Fisher Scientific and used without further purification.

Visible and ultraviolet spectra were obtained on a Varian 2200 spectrophotometer. Circular dichroism experiments were conducted on a Jasco 21-C instrument or a Cary 60 modified by J. Aviv and Associates. All spectroscopic experiments were conducted at 25°. Attempts to study these systems by equilibrium dialysis failed because of the tendency of the highly charged porphyrins to adhere to surfaces. Calorimetric experiments were carried out at 25° in an LKB 10700 batch microcalorimeter equipped with dimethyldichlorosilane treated glass cells. Two milliliter samples of calf thymus DNA (1.4-4.4 mM) were placed in one half-cell and an equal volume of porphyrin solution (0.04-0.16 mM) in the other half-cell. Solutions were at pH 6.8, $\mu = .01 \text{ M}$. Equilibration times ranged from 60 minutes to several hours and observed heat effects were corrected for the heat of dilution of the reactants. After each calorimetric experiment the pH and spectrum of the recovered solution was determined. No pH change was noticed after mixing and spectral features were consistent with complete binding of the porphyrins to DNA. (9) The estimated error in a single calorimetric measurement was estimated as $\pm 1 \text{ kcal/mole}$.

RESULTS AND DISCUSSION

The results of a titration experiment involving H_2TMpyP and poly(dG-dC) at $\mu =$

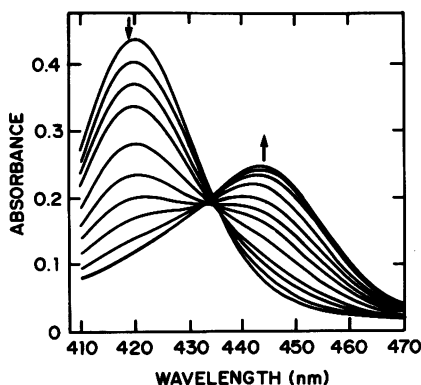


Figure 2. Titration of H_2TMPyP with poly(dG-dC) at $\mu = 0.03$ M. $[H_2TMPyP]_0 = 1.93 \mu M$; $0 \leq [poly(dG-dC)] \leq 57 \mu M$.

0.03 M are shown in Figure 2. The concentration of the porphyrin was $1.93 \mu M$ throughout while the nucleic acid concentration varied from zero to $57 \mu M$. The λ_{max} for the free porphyrin is at 421 nm while that for the complex (H_2TMPyP -poly(dG-dC)) is at 444 nm consistent with our previous findings at $\mu = 0.2$ M (9). The usual procedure for analyzing titration data of this type is to construct r/m vs r plots and extrapolate the linear portion of the resulting curve to $r = 0$ to obtain a value for the inherent binding equilibrium constant, K . In so doing, the data which are emphasized are those obtained in the limit where nearly all of the porphyrin chromophore is bound. We prefer an approach in which an attempt is made to fit all the experimental data using an appropriate model. Equations (1) and (2) have been applied to the titration data and from values of r_{calc} so obtained values of A_{calc} are determined from:

$$A_{calc} = \epsilon_f [P]_0 + (\epsilon_b - \epsilon_f) [DNA]_0 r_{calc} \quad (4)$$

In equation (4), ϵ_f and ϵ_b are the molar absorptivities of the free porphyrin and complexed porphyrin, respectively, at the wavelength under consideration; $[P]_0$ and $[DNA]_0$ are the total concentrations of porphyrin and nucleic acid (in base pairs), respectively. Values of the parameters in equations (1) and (2) are varied systematically using standard computational methods until the best agreement between A_{calc} and A_{exp} is obtained for a given data set. On the basis of earlier work (9) and preliminary plots of r/m vs r , n was set equal to two. Then, for $\omega = 1$, only one parameter remains; the equilibrium constant, K . If we allow for cooperativity ($\omega \neq 1$), then two adjustable parameters are available to fit the data. The equilibrium constants thus obtained are reported to $\pm 10\%$ for each titration at a given wavelength.

Shown in Figure 3 is the result of this analysis as applied to previously published

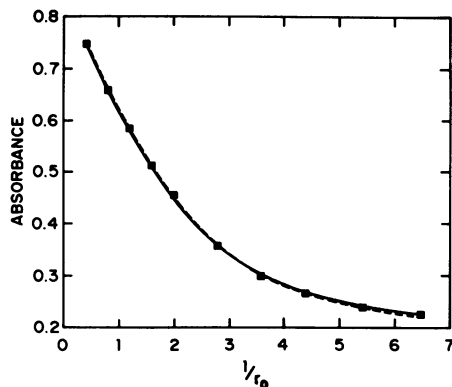


Figure 3. Absorbance at 420 nm of $H_2TMpyP/poly(dG-dC)$ solution as a function of $1/r_0$ ($r_0 \equiv [H_2TMpyP]_0/[poly(dG-dC)]_0$) at $\mu = 0.2$ using data of reference (9). The theoretical curves were obtained via the application of equation (4) with $\epsilon_f = 2.25 \times 10^5 M^{-1} cm^{-1}$ and $\epsilon_b = 5.0 \times 10^4 M^{-1} cm^{-1}$. The best fit for the noncooperative model gives $K = 7.88 \times 10^5 M^{-1}$ (—) while allowing for cooperativity yields $\omega = 0.89$ and $K = 8.65 \times 10^5 M^{-1}$ (- - -).

data at $\mu = 0.2 M$.(9) At the time of publication we claimed that there was no evidence for cooperativity under these conditions and obtained from the standard Scatchard (McGhee-von Hippel) plot that $n = 1.8$ and $K = 7.7 \times 10^5 M^{-1}$. We see that these conclusions are well borne out by the present analysis. The best fit of the data is obtained for $\omega = 0.89$ and $K = 8.65 \times 10^5 M^{-1}$. The theoretical curve for $\omega = 1$ and $K = 7.88 \times 10^5 M^{-1}$ is practically superimposable on the best fit curve. For the experimental conditions considered in the present report, not all the results lend themselves to standard Scatchard analyses whereas the approach taken here, in which all of the data are employed without bias, is uniformly successful.

Figure 4 is the result of the analyses of data at 420 nm at the five sodium ion concentrations considered here. Shown are all the data points and the theoretical curves generated for $\omega = 1$ and $\omega \neq 1$. Representative data analysis at 442 nm are shown in Figure 5 for three of the systems. Once again, a most acceptable fit is achieved for the one and especially the two parameter curve fitting procedure with $n = 2$. A summary of our results is given in Table 1 showing both the non-cooperativity model as well as the best fit of the data allowing for cooperativity.

As may be seen from the results in Table 1 as well as the graphical displays of the analyses in Figures 4 and 5, a definitive case cannot be made for cooperativity in this system, although the situation is less clear at high ionic strengths. We use the results of the one parameter fit to consider the dependence of K on $[Na^+]$; a plot of $\log K_{\omega=1}$ vs. $\log [Na^+]$ is shown in Figure 6. The equation of the line which best fits

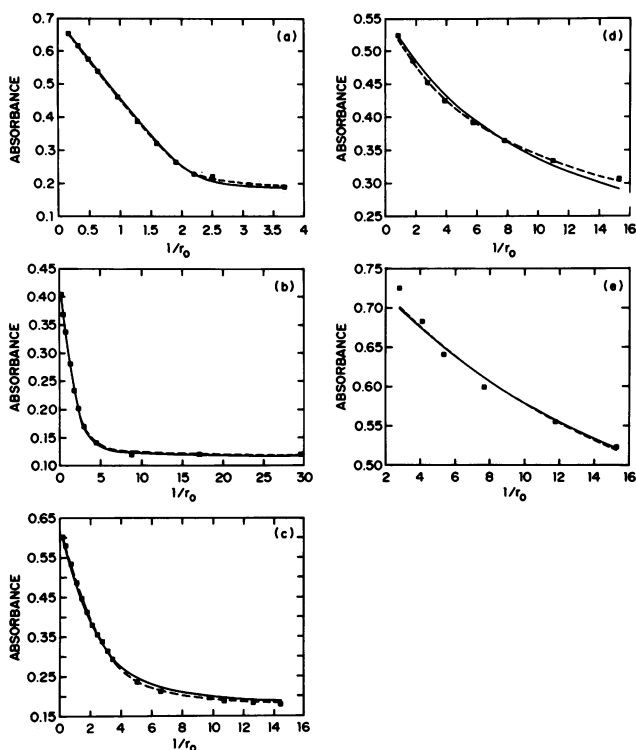


Figure 4. Absorbance at 420 nm of H₂TMpyP/poly(dG-dC) solutions as a function of $1/r_0$ at various sodium ion concentrations. In each case the best fit for the non-cooperative model is shown by (—) while the overall best fit is shown by (---). (a) $[Na^+] = 0.01$, $\epsilon_f = 2.26 \times 10^5 M^{-1} cm^{-1}$; $\epsilon_b = 5.9 \times 10^4 M^{-1} cm^{-1}$; $K_{\omega=1} = 2.77 \times 10^7 M^{-1}$; $\omega = 2.4$, $K = 5.50 \times 10^6 M^{-1}$. (b) $[Na^+] = 0.03$, $\epsilon_f = 2.26 \times 10^5 M^{-1} cm^{-1}$; $\epsilon_b = 6.0 \times 10^4 M^{-1} cm^{-1}$; $K_{\omega=1} = 3.44 \times 10^6 M^{-1}$; $\omega = 1.2$, $K = 2.79 \times 10^6 M^{-1}$. (c) $[Na^+] = 0.1$, $\epsilon_f = 2.26 \times 10^5 M^{-1} cm^{-1}$; $\epsilon_b = 6.0 \times 10^4 M^{-1} cm^{-1}$; $K_{\omega=1} = 6.35 \times 10^5 M^{-1}$; $\omega = 0.53$, $K = 9.32 \times 10^5 M^{-1}$. (d) $[Na^+] = 0.3$, $\epsilon_f = 2.26 \times 10^5 M^{-1} cm^{-1}$; $\epsilon_b = 6.0 \times 10^4 M^{-1} cm^{-1}$; $K_{\omega=1} = 5.52 \times 10^4 M^{-1}$; $\omega = 5.1$, $K = 3.65 \times 10^4 M^{-1}$. (e) $[Na^+] = 1.0$, $\epsilon_f = 2.26 \times 10^5 M^{-1} cm^{-1}$; $\epsilon_b = 6.4 \times 10^4 M^{-1} cm^{-1}$; $K_{\omega=1} = 1.72 \times 10^4 M^{-1}$, $\omega = 0$, $K = 1.86 \times 10^4 M^{-1}$.

these points is:

$$\log K_{\omega=1}^{calc} = 4.10 - 1.64 \log [Na^+] \quad (5)$$

The values of $K_{\omega=1}$ shown in Table 1 were obtained from this equation. Note that the equilibrium constant derived from the titration data at $[Na^+] = 0.2 M$ obtained earlier (9) is significantly removed from this linear plot but that the value of K obtained at these conditions from relaxation data (12) is practically on the line. We have no explanation for this discrepancy at present. The results summarized in equation (5) can be used to calculate the quantity z in equation (3). Wilson and coworkers (6,7)

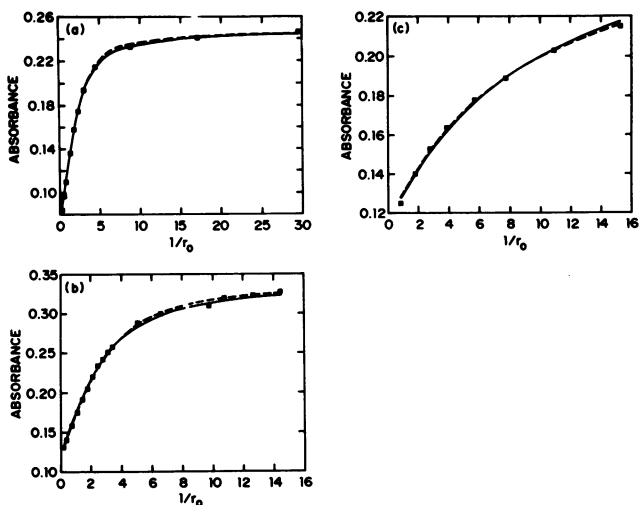


Figure 5. Absorbance at 442 nm of $H_2TMpyP/poly(dG-dC)$ solutions as a function of $1/r_0$ at various sodium ion concentrations. In each case the best fit for the noncooperative model is shown by (—) while the overall best fit is shown by (- - - -). (a) $[Na^+] = 0.03$ $\epsilon_f = 3.7 \times 10^4 M^{-1} cm^{-1}$; $\epsilon_b = 1.3 \times 10^5 M^{-1} cm^{-1}$; $K_{\omega=1} = 1.01 \times 10^6 M^{-1}$; $\omega = 0.75$, $K = 1.24 \times 10^6 M^{-1}$ (b) $[Na^+] = 0.1$ $\epsilon_f = 4.4 \times 10^4 M^{-1} cm^{-1}$; $\epsilon_b = 1.18 \times 10^5 M^{-1} cm^{-1}$; $K_{\omega=1} = 3.47 \times 10^5 M^{-1}$; $\omega = 0.61$, $K = 4.32 \times 10^5 M^{-1}$. (c) $[Na^+] = 0.3$ $\epsilon_f = 4.7 \times 10^4 M^{-1} cm^{-1}$; $\epsilon_b = 1.10 \times 10^5 M^{-1} cm^{-1}$; $K_{\omega=1} = 5.96 \times 10^4 M^{-1}$; $\omega = 1.9$, $K = 5.30 \times 10^4 M^{-1}$.

have estimated ϕ and ϕ^* as 0.88 and 0.82 respectively in a sodium chloride medium leading to an estimate of z as 1.7. Thus, if the model leading to equation (3) is applicable here, the implication is that intercalated H_2TMpyP forms only two ion-pair

Table 1
Results of Titration Experiments Involving H_2TMpyP and $poly(dG-dC)$

$[Na^+]$	λ	$K_{\omega=1}$	$K_{\omega=1}^{calc}$	ω	$K (M^{-1})$
0.01	420	2.77×10^7	2.40×10^7	2.4	5.50×10^6
0.03	420	3.44×10^6	3.96×10^6	1.2	2.79×10^6
	442	1.01×10^6		.75	1.24×10^6
0.1	420	6.35×10^5	5.50×10^5	.53	9.32×10^5
	442	3.47×10^5		.61	4.32×10^5
0.3	420	5.52×10^4	9.07×10^4	5.1	3.65×10^4
	442	5.96×10^4		1.9	5.30×10^4
1.0	420	1.72×10^4	1.26×10^4	-	-

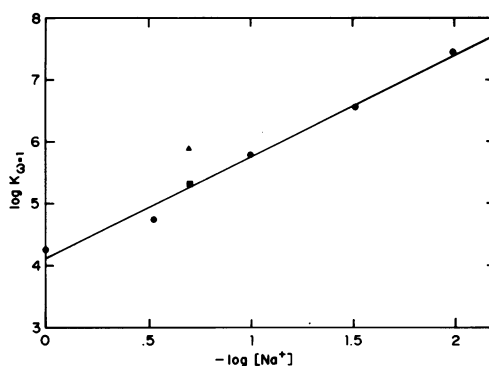


Figure 6. Plot of $\log K_{0=1}$ vs $-\log [\text{Na}^+]$. The data of the present report is shown as (●). The results of the titration data of reference (9) are shown as (▲) while the value of K obtained from relaxation data (cf. reference 12) is shown as (■).

contacts in the complex although its formal charge is +4. Indeed, when a model of the intercalated porphyrin is constructed, not all of the N-methylpyridyl groups form contacts with phosphate moieties.

The influence of $[\text{Na}^+]$ (or ionic strength for the 1:1 electrolyte, NaCl) on the interactions of H_2TMpyP with calf thymus DNA was studied at $1/r_0 \geq 50$ using visible absorption and circular dichroism methods. A typical result in the standard absorption mode is shown in Figure 7. Solution (a), for which $\mu = .0040$ has a λ_{max} at 437 nm; (b) for which $\mu = .052$ has a λ_{max} at 436 nm; (c) with $\mu = 0.50$ has a λ_{max} at 430 nm while (d) for which $\mu = 2.0$ has a λ_{max} at 424 nm. Solution (e) is at the same conditions as (d) except that no DNA has been added. The λ_{max} for this solution is at 423.4 nm. There is a very slight dependence of λ_{max} and molar absorptivity of H_2TMpyP on ionic strength even in the absence of DNA but these cannot account for the results shown in Figure 7. At $\mu = 0.01$ M $\lambda_{\text{max}} = 421.4$ nm and $\epsilon = 2.3 \times 10^5 \text{ M}^{-1} \text{ cm}^{-1}$ compared to values of 423.4 nm and $\epsilon = 2.5 \times 10^5 \text{ M}^{-1} \text{ cm}^{-1}$ at $\mu = 2.0$ M. As implied from the results of Figure 5, the spectrum of the H_2TMpyP -poly(dG-dC) complex is not ionic strength dependent with $\lambda_{\text{max}} \sim 444$ nm and $\epsilon \sim 1.3 \times 10^5 \text{ M}^{-1} \text{ cm}^{-1}$ for a $0.03 \leq \mu \leq 0.3$. Similarly, the spectrum of the H_2TMpyP -poly(dA-dT) complex has $\lambda_{\text{max}} \sim 430$ nm and $\epsilon = 2.0 \times 10^5 \text{ M}^{-1} \text{ cm}^{-1}$ under conditions of $0.01 \leq \mu \leq 0.5$. Therefore, we conclude that the effects that are illustrated in Figure 7 reflect changes in H_2TMpyP /DNA interactions. As pointed out in the Introduction, large bathochromic shifts of the Soret maximum with significant hypochromicity are characteristic of H_2TMpyP intercalation in GC-rich regions while a $\lambda_{\text{max}} \sim 430$ nm with modest hypochromicity reflects 'external' binding to AT-rich regions. Absorbance changes similar to those observed for H_2TMpyP bound to calf thymus DNA are seen for H_2TMpyP binding to *Escherichia coli*

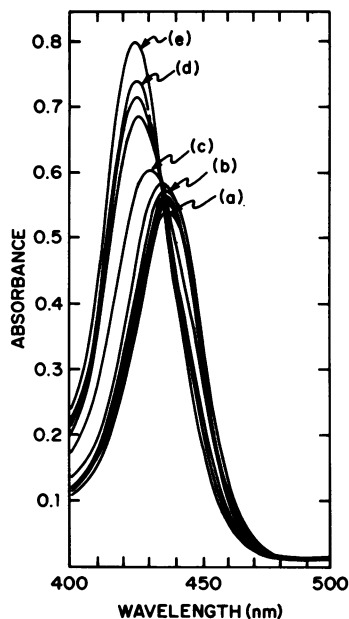


Figure 7. Absorbance of solutions containing 3.1 μM H_2TMpyP and 211 μM calf thymus DNA as a function of μ . (a) $\mu = .0040 \text{ M}$, (b) $\mu = .052 \text{ M}$, (c) $\mu = .50 \text{ M}$, (d) $\mu = 2.0 \text{ M}$. Curve (e) is at the same conditions as curve (d) except no calf thymus DNA has been added.

DNA when the ionic strength is varied. This latter DNA, like calf thymus DNA, is a natural DNA with about equal GC and AT base pair content but of different base sequence. On this basis, we present as our model the suggestion that in these polymers of mixed base pair content there are regions of GC base pairs and AT base pairs which maintain the properties seen in their respective homopolymers (this will be substantiated, *vide infra*, by CD results) and that the base specificity of H_2TMpyP to these mixed polymers depends on bulk ionic strength with GC preference at low μ , converting to AT preference as μ is increased. Analysis of these results must also include the tendency of the porphyrin to dissociate from the polymer as the ionic strength increases. As a simplest model, the absorbance of a solution at some given wavelength can be written as:

$$A = \epsilon_{\text{f}}[\text{P}] + \epsilon_{\text{GC}}[\text{P}\cdot\text{GC}] + \epsilon_{\text{AT}}[\text{P}\cdot\text{AT}] \quad (6)$$

where P·GC represents the porphyrin chromophore intercalated in GC-rich regions of DNA and P·AT represents H_2TMpyP externally bound to AT-rich regions. Interface regions in the natural DNA have been neglected and furthermore we use for ϵ_{GC} and ϵ_{AT} the molar absorptivities of the porphyrin when bound to the synthetic

Table 2
Distribution of H₂TMpyP as a Function of Ionic Strength
[H₂TMpyP]₀ = 3.1 μM; [DNA]₀ = 210 μM; T° = 25°C

μ	% GC ^{Abs} _{calc}	% GC ^{CD} _{calc}	% AT	% Free
0.0040	82	86	13	5
0.012	78	79	16	6
0.052	71	68	24	5
0.2	60	43	31	10
0.5	46	32	26	28
1.0	23	22	38	38
2.0	12	14	39	50

polynucleotides poly(dG-dC) and poly(dA-dT), respectively. We also take advantage of the fact that at 440 nm, $\epsilon_{GC} = \epsilon_{AT} = \epsilon_D$ so at this wavelength

$$A_{440} = \epsilon_f[P] + \epsilon_D([P]_0 - [P]) \quad (7)$$

with $\epsilon_D = 1.3 \times 10^5 \text{ M}^{-1}\text{cm}^{-1}$. Applying equations (6) and (7) to the data of Figure 7 permits a determination of the fraction of the porphyrin bound at GC and AT regions respectively at various ionic strengths (cf Table 2).

To further test this model, we determined the induced circular dichroism spectra in the Soret region for H₂TMpyP/DNA solutions as a function of ionic strength (see Figure 8). At $\mu = .0040 \text{ M}$ (curve "a" in Figure 8) a negative feature is obtained

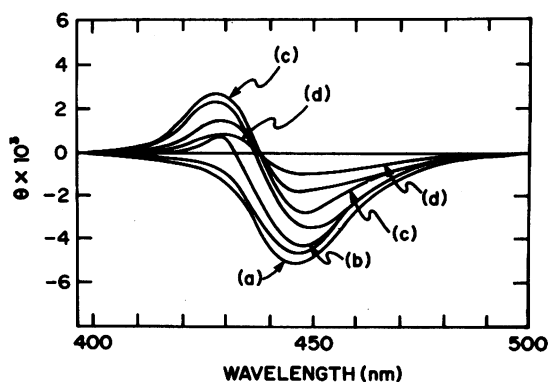


Figure 8. Induced circular dichroism spectra in the Soret region for the solutions described in Figure 7.

centered at 446 nm thereby resembling the induced CD of H₂TMpyP/poly(dG-dC) solutions. When the ionic strength is raised to 0.052 M (curve "b"), a small positive feature develops at 430 nm corresponding to the characteristic positive band of H₂TMpyP/poly(dA-dT) mixtures. By $\mu = 0.50$ M (curve "c") this 430 nm positive band has become quite prominent although the long-wavelength negative band is still a major feature of the spectrum. At $\mu = 2.0$ M (curve "d"), the negative band has all but disappeared and only a positive feature at 430 nm remains. It might be noted that the total intensity of the CD spectrum at $\mu = 2.0$ M has diminished significantly from that obtained at $\mu = 0.50$ M. A considerable fraction of H₂TMpyP has dissociated from the polymer at $\mu = 2.0$ M (cf. Table 2) and unbound H₂TMpyP being nonchiral shows no circular dichroism spectrum. Thus the CD results corroborate the conclusion drawn from absorbance measurements, i.e., the porphyrin base specificity changes with ionic strength. An analysis of the data was attempted to determine the porphyrin distribution. The wavelength chosen was 450 nm where H₂TMpyP·poly(dG-dC) has a significant negative feature while the molar ellipticity of H₂TMpyP·poly(dA-dT) is near zero. At no wavelength is the converse true, i. e., that $|\theta_M|$ is large for H₂TMpyP·poly(dA-dT) and zero for the poly(dG-dC) complex. Therefore, we employ the data of Figure 8 to obtain the percent porphyrin bound to GC-rich regions of calf thymus DNA using the spectrum of H₂TMpyP·poly(dG-dC) as a standard. The results are included in Table 2 as a comparison to the visible absorption results. Given the various approximations in these analyses the agreement seems entirely satisfactory.

Calorimetric studies have been conducted with CuTMpyP, ZnTMpyP and H₂TMpyP and calf thymus DNA at $\mu = .01$ M. According to the model presented by us earlier (9), CuTMpyP is expected to be an intercalator and GC-specific, while ZnTMpyP is a non-intercalator and is AT-specific. We have determined that $\Delta H^\circ = -5.9$ kcal/mole for CuTMpyP and $\Delta H^\circ = +1.5$ kcal/mole for ZnTMpyP, values which are characteristic of intercalators and nonintercalators, respectively (13). For H₂TMpyP under the same conditions, we obtain $\Delta H^\circ = -4.6$ kcal/mole. If we consider the enthalpy values for CuTMpyP and ZnTMpyP at $\mu = 0.01$ M as standards for intercalation at GC and interaction at AT sites, respectively, we calculate that under these conditions, H₂TMpyP is distributed as 82% at GC-sites and 18% at AT-sites. Comparison with the results in Table 2 show close agreement between the calorimetric and spectroscopic results.

We proceed to define a parameter $\rho_K = K_{AT}/K_{GC}$ where $K_{AT} = [H_2TMpyP \cdot AT]/[H_2TMpyP][AT]$ and $K_{GC} = [H_2TMpyP \cdot GC]/[H_2TMpyP][GC]$. Thus $\rho_K = [H_2TMpyP \cdot AT][GC]/[H_2TMpyP \cdot GC][AT]$. Because the ratio of porphyrin to nucleic acid base pairs is small in these experiments, we estimate $[GC]/[AT]$ as 0.72, the value in native calf thymus DNA (14). Therefore, $\rho_K \sim 0.72 [H_2TMpyP \cdot AT]/[H_2TMpyP \cdot GC]$.

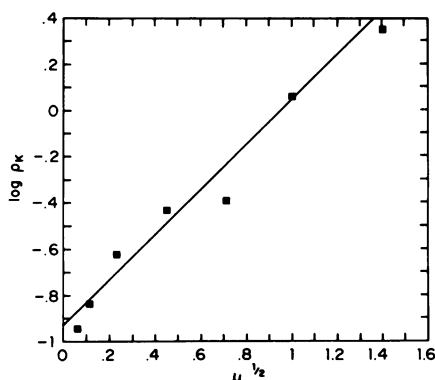


Figure 9. Distribution of H₂TMpyP as a function of ionic strength. See text for definition of ρ_K .

Figure 9 shows a plot of $\log \rho_K$ vs. $\mu^{1/2}$ as a graphical display of the change in base specificity of H₂TMpyP with ionic strength. As may be seen from this figure, the plot is somewhat scattered but appears to be linear with a slope of unity. Although there is no explicit theory to account for this dependence it is reminiscent of those obtained for Debye-Hückel type interactions.

Theories which have been developed for the influence of ionic strength on binding of ligands to homopolymers are inadequate to account for these effects. Indications of similar findings exist in the literature but the results are less definitive than those presented here. Norden and Tjerneld have shown that the CD spectrum of the methylene blue/DNA complex shows a "remarkable dependence" on ionic strength changing sign from negative to positive with increasing sodium ion concentration (15). They have interpreted their results as reflecting two types of intercalation modes for methylene blue with one mode favored at low ionic strength and the other at high. Changes in DNA conformation in the range 0.1 to 1 M NaCl have been suggested by Giartosio et al. (16) as the basis for fluorescence effects observed for the bisbenzimidazole/DNA system. The unifying notion in these studies and the present one is that not only the avidity but the nature of polyelectrolyte small molecule interactions may well be very sensitive to the bulk ionic strength. Future efforts will expand on these studies to include the binding of porphyrins to poly(dA-dT). In this manner we hope to determine the factors responsible for the dependence of base specificity on ionic strength.

ACKNOWLEDGMENT

Grant support from the National Institutes of Health (Grant GM34676) is gratefully acknowledged.

*To whom correspondence should be addressed.

REFERENCES

1. McGhee, J.D. and von Hippel, P.H. (1974) *J. Mol. Biol.* **86**, 469-489.
2. Friedman, R.A.G. and Manning, G.S. (1984) *Biopoly.* **23**, 2671-2714.
3. Wilson, W.D. and Jones, R.L. (1982) in Intercalation Chemistry, Academic Press, New York, N.Y. pp. 445-500.
4. Manning, G.S. (1969) *J. Chem. Phys.* **51**, 924-933 .
5. Manning, G.S. (1978) *Quart. Rev. Biophys.* **11**, 179-246.
6. Wilson, W.D. and Lopp, I.G. (1979), *Biopoly.* **18**, 3025-3041.
7. Wilson, W.D. Kirshnamoorthy, C.R., Wang, Y.-H. and Smith, J.C. (1985) *Biopoly.* **24**, 1941-1961.
8. Fiel, R.J., Howard, J.C., Mark, E.H. and Dattagupta, N. (1979) *Nucl. Acids Res.* **6**, 3093-3118.
9. Pasternack, R.F., Gibbs, E.J. and Villafranca, J.J. (1983) *Biochem* **22**, 2406-2414.
10. Müller, W. and Crothers, D.M. (1968) *J. Mol. Biol.* **35**, 251-290.
11. Wells, R.D., Larson, J.E., Grant, R.C., Shortle, B.E. and Cantor, C.R. (1970) *J. Mol. Biol.* **54**, 465-497.
12. Pasternack, R.F., Gibbs, E.J. and Villafranca, J.J. (1983) *Biochem* **22**, 5409-5417.
13. Quadrifoglio, F., Ciana, A. and Crescenzi, V. (1976) *Biopoly.* **15**, 595-597.
14. Müller, W., Crothers, D.M. and Waring, M.J. (1973) *Eur. J. Biochem.* **39**, 223-234.
15. Norden, B. and Tjernelund, F. (1982) *Biopoly.* **21**, 1713-1734.
16. Giartosio, A., Ferraro, A., Lavaggi, M.V., Allegra, P. and Turano, C. (1984) *Physiol. Chem. Phys. Med. NMR* **16**, 481-490.